

Integrated spiral waveguide amplifiers on erbium-doped thin-film lithium niobate

Xiongshuo Yan*,¹ Yi'an Liu*,¹ Jiangwei Wu,¹ Yuping Chen,^{1, a)} and Xianfeng Chen^{1, b)}
*State Key Laboratory of Advanced Optical Communication Systems and Networks,
 School of Physics and Astronomy, Shanghai Jiao Tong University, Shanghai 200240,
 China*

(Dated: 1 February 2022)

Integrated optical amplifiers and light sources are of great significance for photonic integrated circuits (PICs) and have attracted many research interests. Doping rare-earth ions in materials as a solution to realize efficient optical amplifiers and lasing has been investigated a lot. We investigate the erbium-doped lithium niobate on insulator (LNOI). Here, spiral waveguide amplifiers were fabricated on a 1-mol% erbium-doped LNOI by CMOS-compatible technique. We demonstrated a maximum internal net gain of 8.3 dB at 1530 nm indicating a net gain per unit length of 15.6 dB/cm with a compact spiral waveguide of 5.3 mm length and ~ 0.06 mm² footprint. The erbium-doped integrated lithium niobate spiral waveguide amplifiers would pave the way in the PICs of the lithium niobate platform, especially in achieving efficient integration of active and passive devices on a lithium niobate thin film, which will make full use of its excellent physical properties such as remarkable photoacoustic, electro-optic, and piezoelectric characteristics.

Integration is of great significance in device miniaturization and improving energy efficiency¹. Photonic integrated circuits as one of important goals for the development of photonics have attracted enormous attentions and became one of the most investigated research fields. Lithium niobate (LN) as an emerging integrated photonic platform material is widely used in optical and microwave fields, due to its rich properties as wide transparent wavelength range, excellent electro-optic, acousto-optic characteristics and large second-order nonlinear susceptibility². In particular, with the lithium niobate on insulator (LNOI) commercializing, more compact and low-cost photonic devices with high-performance can be achieved on LNOI, which is very important for the Photonic integrated circuits, especially for the development of a large number of integrated functional devices³⁻⁵. Many on-chip optical devices based on LNOI have been demonstrated, such as efficient frequency converters⁶⁻¹⁰, electro-optical modulators¹¹⁻¹⁴, frequency comb source¹⁵⁻¹⁷. However, for a complete photonic integrated circuits, integrated waveguide amplifiers and light sources are essential elements to realize on-chip various functionalities. Due to the LN is not a efficient gain medium, we can not achieve waveguide amplifier and lasing directly on a LNOI. In order to overcome this shortage, the most straightforward approaches is to doping rare earth ions into the LNOI, which is similar to the erbium doped fiber amplifier. Actually, erbium-doped laser and waveguide amplifier have been realized in many host materials and show great potential for integrated waveguide amplifiers and light sources¹⁸⁻²³. The on-chip whispering gallery mode lasers based on the LNOI also have been demonstrated, recently²⁴⁻²⁸. But, there are still less research works about the on-chip

amplifiers based on the LNOI. It's worth noting that a efficient waveguide amplifier based on erbium-doped thin film LN has been realized recently²⁹. However, this straight waveguide amplifier with a length of 5-mm is still too long to realize a more compact on-chip photonic integration, especially for a chip with a large number of functional devices.

Here, we demonstrated a spiral waveguide amplifier with a maximum net gain of 8.3 dB on a 1-mol% erbium-doped LNOI, with a 15.6 dB/cm net gain per unit length. The spiral waveguide amplifiers with total 5.3-mm-long and ~ 0.06 mm² of footprint based on the CMOS compatible process, presents strong light confinement for the signal and pump light and have great significance on photonic integrated circuits. We shows that it is possible to achieve efficient on-chip amplifiers with a small footprint spiral waveguides, which would pave the way for the active and passive photonic devices integration of various functionalities on the erbium-doped LNOI platform.

The spiral waveguide amplifiers were fabricated on a 1-mol % Z-cut erbium-doped LNOI, with 600-nm-thick erbium-doped lithium niobate (LN), 2- μ m-thick silica (SiO₂) and 500- μ m-thick silicon (Si) substrate [Fig. 1(a)]. Here, we select the lithium niobate (LiNbO₃) as a host materials due to its excellent physical properties compared to other materials. In order to obtain uniform erbium ions doping concentration and achieve a better gain effect, we doped erbium ions into LN during the crystal growth processes²⁴.

Figure 1(b) shows the scanning electron microscope (SEM) image of the spiral waveguide amplifier. The total length of the spiral waveguide amplifier is 5.3 mm with a minimum radius of 25 μ m in the bend part of the spiral waveguides. The footprint of the whole spiral waveguide is ~ 0.06 mm², which is the smallest among all erbium-doped LNOI waveguide amplifiers²⁹⁻³¹, to the best of our knowledge. Since it will be more suitable for the compact on-chip integration. Insets in Fig. 1(b) are

^{a)}Electronic mail: ypchen@sjtu.edu.cn

^{b)}Electronic mail: xfchen@sjtu.edu.cn

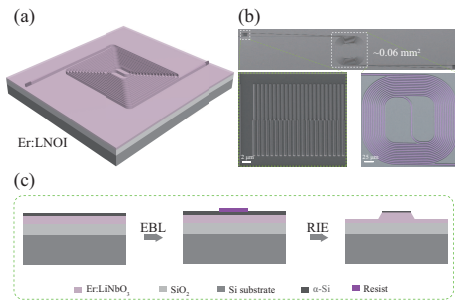


FIG. 1. Schematic of the spiral waveguide amplifiers and its brief fabrication processes. (a) A spiral waveguide amplifier on an erbium-doped LNOI. (b) Scanning electron microscope (SEM) images of the whole spiral waveguide amplifier, and the magnified coupling grating and spiral waveguide with false-color. (c) The brief fabrication processes of spiral waveguide amplifiers. EBL: electron beam lithography, RIE: reactive ion etching.

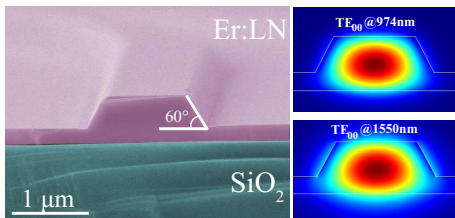


FIG. 2. The false-color SEM image of the fabricated spiral waveguide cross-section and simulated electric field distributions of the TE_{00} modes at 1550 nm and 974 nm. The top width of spiral waveguide is $1 \mu\text{m}$, with the thickness around 350 nm and a sidewall angle of $\sim 60^\circ$

the magnified grating and spiral waveguides part SEM image with false color. In order to obtain high coupling efficiency for pump and signal light. The coupling grating is designed to be two part with periods as 900nm for 1550 nm (Top, duty cycle 0.33) and $1.05 \mu\text{m}$ for 980 nm (bottom, duty cycle 0.46).

The brief fabrication processes of spiral waveguide amplifiers are shown in Fig. 1 (c). Mainly fabrication details including five steps: (1) a 600-nm thick amorphous silicon was deposited as a hard etching mask, (2) a layer of resist was spin-coated onto the Er:LNOI, (3) the spiral waveguide structure was patterned via electron-beam lithography (EBL), (4) the mask layer patterns was transferred to the Er:LN layer with an Ar^+ plasma etching process and (5) the residual mask was removed by wet etching.

Figure 2 shows the cross sections of the spiral waveguide (left) and simulated electric field distributions of the TE_{00} modes (right) at pump and signal wavelength. The fabricated spiral waveguides have a top width of $1 \mu\text{m}$, a thickness of 350-nm, and a sidewall angle of $\sim 60^\circ$, shown as the waveguide cross-section SEM image. From the electric field distribution we find that the micron-scale waveguides can support strong light confinement. The transverse electric (TE) modes are selected both for

the pump (980 nm) and signal (C-band) wavelength.

Figure (3) shows the experimental setup for the characterization of the spiral waveguide amplifier net gain. The spiral waveguide amplifier was pumped by two 980-nm laser sources (LR-MFJ-980, actual output wavelength at 974 nm) from both the input and output sides. A continuous-wave (CW) telecom tunable laser (New Focus TLB-6728, linewidth ≤ 200 kHz, 1520-1570 nm) was combined by a wavelength division multiplexer (WDM) and coupled into the spiral waveguide from one side. The in-line polarization controllers were used to make the TE polarization light coupling into the device. Then, the output light was collected by an optical spectrum analyzer (OSA) from the 1550 port of the WDM. The top inset shows the photograph of the spiral waveguide amplifier pumped by 974 nm light with strong up-conversion induced green photoluminescence. The bottom inset in Fig. 3 shows the optical microscope image of the small footprint spiral waveguide amplifier comparing with a single-mode optical fiber (Coning SMF-28).

We characterized the propagation losses of the spiral waveguide amplifier at the signal wavelength (1550 nm) by a microring. Figure (4) shows the SEM image of the microring with the top width of $1 \mu\text{m}$ and radius of $30 \mu\text{m}$, which exhibits the loaded and intrinsic Q factor of 5×10^4 and 5.4×10^4 , respectively. We can estimate the propagation loss α of the spiral waveguide based on the equation $\alpha = 2\pi n_{eff}/\lambda_0 Q_I$, where n_{eff} is the effective index of the waveguide and λ_0 is the target wavelength. The calculated propagation loss at 1550 nm is $\sim 6.86\text{dB/cm}$, which lead to a loss about 3.64 dB for our 5.3-mm spiral waveguide amplifiers. We also measured the coupling loss of our coupling grating at 980 nm and 1550 nm, which are 16 dB and 13.4 dB, respectively. The launched pump and signal powers into the spiral waveguide have been calibrated by using the above measurement results.

Figure 5(a) presents the measured signal spectra at 1530 nm with the increasing pump power, which shows the apparently signal enhancement. Figure 5(b) is the amplifier net gain as a function of the launched pump power with different signal powers at 1530 nm. As expected, the spiral waveguide optical gain increases rapidly at the small pump powers. Then, we can observe the gain approaching saturation with the launched pump power increasing around 10 mW. A maximum net internal gain of 8.3 dB is achieved with the signal power at -10.7dBm and pump power at 10.78 mW, which corresponding to a net gain per unit length of ~ 15.6 dB/cm. It is higher than other erbium-doped LNOI²⁹ and bulk LN^{32,33}. What's more, a small gain saturation is also found when the launched signal power increasing, shown as Fig. 5(c). The net gain at other wavelengths of telecommunication bands is characterized as shown in Fig. 5(d), with a launched signal power at -10.7 dbm. The pink area of Fig. 5(d) shows the net gain over 3 dB and we can find that the spiral waveguide amplifier exhibits a net gain bandwidth of 1530-1570 nm. These re-

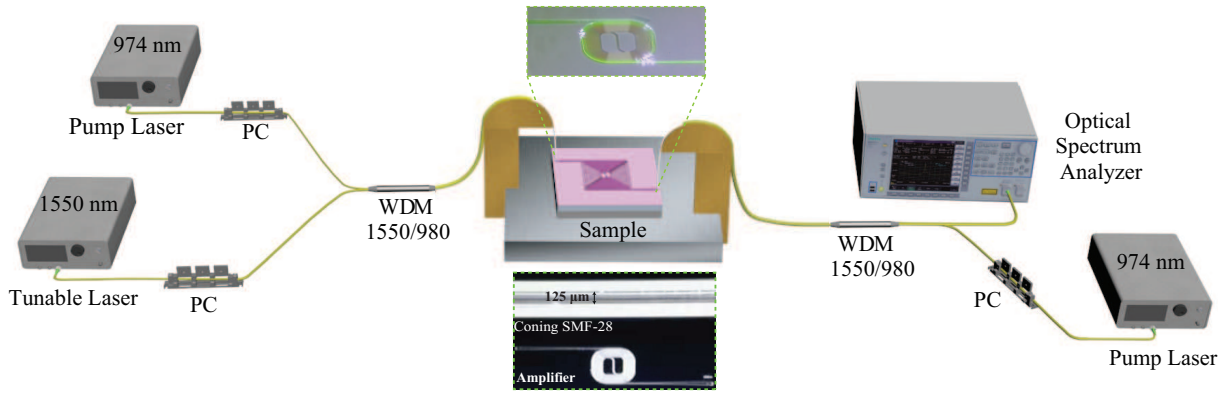


FIG. 3. The net gain measurement setup. Insets are the microscope photograph of the spiral waveguide amplifiers pumped by 974 nm light with strong up-conversion induced green photoluminescence (Top) and the optical microscope image of the spiral waveguide amplifier comparing with a single-mode optical fiber (Coning SMF-28) (bottom).

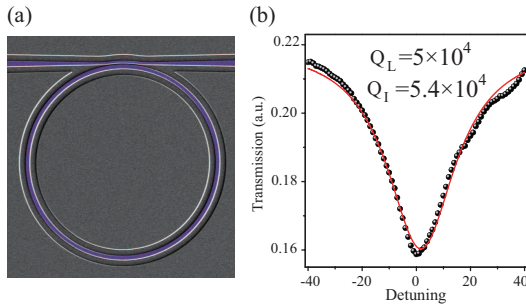


FIG. 4. Propagation loss measurement with a micro-ring. (a) The false-color SEM image of microring with the radius of 30 μm . (b) The Lorentzian fitting exhibiting the microring with a loaded Q factor of $Q_L = 5 \times 10^4$ and intrinsic Q factor of $Q_I = 5.4 \times 10^4$.

sults show the potential for on-chip integration with high optical gain amplifier in erbium-doped LNOI platform.

In conclusion, we fabricated high-gain optical spiral waveguide amplifiers with total 5.3-mm-long and $\sim 0.06 \text{ mm}^2$ of areas on a 1-mol% erbium-doped LNOI. A maximum internal net gain of 8.3 dB at 1530 nm and a broad gain band (1530-1570 nm) have been demonstrated. A maximum net gain per unit length can reach up to 15.6 dB/cm. The strong confinement to the pump and signal light, small footprint and relative high signal enhancement of the spiral waveguide amplifier are of great significance for the LN on-chip photonic integrated circuits, which would pave the way in the photonic integrated circuits of lithium niobate platform or the hybrid integration.

It is worth noting that another two erbium-doped waveguide amplifiers works were posted on arXiv^{30,31}, during the preparation of this article. Comparing to these two works, our spiral waveguide amplifiers have a narrower top width and smallest footprint, which means the spiral waveguide amplifiers are integrated and can support more compact on-chip integration. Spiral wave-

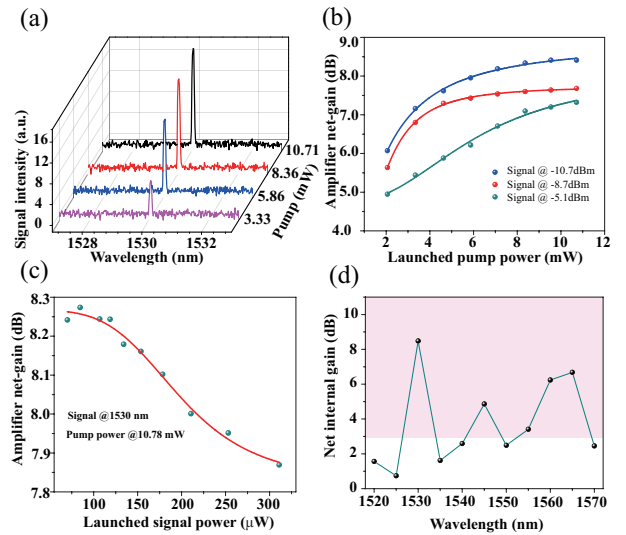


FIG. 5. Gain characterization of spiral waveguide amplifiers. (a) Measured signal spectra as a function of launched pump power at 1530 nm. (b) Measured net internal gain at different launched signal powers (1530 nm) as a function of launched pump power. (c) Measured net internal gain as a function of launched 1530 nm signal powers with a fixed pump powers at 10.78 mW. (d) Net internal gain as a function of signal wavelength with a fixed signal and pump power at -10.7 dBm and 10.78 mW, respectively.

guide amplifiers should be better for a large number of photonic devices integration.

This work was supported by the National Key R & D Program of China (Grant Nos. 2019YFB2203501, and 2017YFA0303701, 2018YFA0306301), the National Natural Science Foundation of China (Grant Nos. 91950107, 11734011), Shanghai Municipal Science and Technology Major Project (2019SHZDZX01-ZX06), and SJTU No. 21X010200828.

We thank Dr. Hao Li for providing ICP-RIE etching help for this device.

[*] These authors contributed equally to this Letter.

- ¹J. D. Bradley and M. Pollnau, “Erbium-doped integrated waveguide amplifiers and lasers,” *Laser & Photonics Reviews* **5**, 368–403 (2011).
- ²D. N. Nikogosyan, *Nonlinear optical crystals: a complete survey* (Springer Science & Business Media, 2006).
- ³A. Boes, B. Corcoran, L. Chang, J. Bowers, and A. Mitchell, “Status and potential of lithium niobate on insulator (lnoi) for photonic integrated circuits,” *Laser & Photonics Reviews* **12**, 1700256 (2018).
- ⁴J. Lin, F. Bo, Y. Cheng, and J. Xu, “Advances in on-chip photonic devices based on lithium niobate on insulator,” *Photonics Research* **8**, 1910–1936 (2020).
- ⁵M. Zhang, C. Wang, R. Cheng, S. A. Amirhassan, and L. Marko, “Monolithic ultrahigh-q lithium niobate microring resonator,” *Optica* **4**, 1536– (2017).
- ⁶R. Luo, Y. He, H. Liang, M. Li, and Q. Lin, “Highly tunable efficient second-harmonic generation in a lithium niobate nanophotonic waveguide,” *Optica* **5**, 1006–1011 (2018).
- ⁷X. Ye, S. Liu, Y. Chen, Y. Zheng, and X. Chen, “Sum-frequency generation in lithium-niobate-on-insulator microdisk via modal phase matching,” *Optics Letters* **45**, 523–526 (2020).
- ⁸L. Ge, Y. Chen, H. Jiang, G. Li, B. Zhu, X. Chen, *et al.*, “Broadband quasi-phase matching in a mgo:pln thin film,” *Photonics Research* **6**, 954–958 (2018).
- ⁹J. Lin, Y. Xu, J. Ni, M. Wang, Z. Fang, L. Qiao, W. Fang, and Y. Cheng, “Phase-matched second-harmonic generation in an on-chip l i n b o 3 microresonator,” *Physical Review Applied* **6**, 014002 (2016).
- ¹⁰J. Lin, N. Yao, Z. Hao, J. Zhang, W. Mao, M. Wang, W. Chu, R. Wu, Z. Fang, L. Qiao, *et al.*, “Broadband quasi-phase-matched harmonic generation in an on-chip monocrystalline lithium niobate microdisk resonator,” *Physical Review Letters* **122**, 173903 (2019).
- ¹¹M. Xu, M. He, H. Zhang, J. Jian, Y. Pan, X. Liu, L. Chen, X. Meng, H. Chen, Z. Li, *et al.*, “High-performance coherent optical modulators based on thin-film lithium niobate platform,” *Nature communications* **11**, 1–7 (2020).
- ¹²M. Li, J. Ling, Y. He, U. A. Javid, S. Xue, and Q. Lin, “Lithium niobate photonic-crystal electro-optic modulator,” *Nature Communications* **11**, 1–8 (2020).
- ¹³C. Wang, M. Zhang, X. Chen, M. Bertrand, A. Shams-Ansari, S. Chandrasekhar, P. Winzer, and M. Loncar, “Integrated lithium niobate electro-optic modulators operating at cmos-compatible voltages,” *Nature* **562**, 101–104 (2018).
- ¹⁴B. Pan, J. Hu, Y. Huang, L. Song, J. Wang, P. Chen, L. Liu, and D. Dai, “The first demonstration of high-speed linbo3 thin-film optical modulators operating at the wavelength of 2 μm ,” in *Asia Communications and Photonics Conference* (Optical Society of America, 2020) pp. M4D–7.
- ¹⁵C. Wang, M. Zhang, M. Yu, R. Zhu, H. Hu, and M. Loncar, “Monolithic lithium niobate photonic circuits for kerr frequency comb generation and modulation,” *Nature Communications* **10**, 1–6 (2019).
- ¹⁶Z. Fang, H. Luo, J. Lin, M. Wang, J. Zhang, R. Wu, J. Zhou, W. Chu, T. Lu, and Y. Cheng, “Efficient electro-optical tuning of an optical frequency microcomb on a monolithically integrated high-q lithium niobate microdisk,” *Optics Letters* **44**, 5953–5956 (2019).
- ¹⁷Y. He, Q. F. Yang, J. Ling, R. Luo, and Q. Lin, “Self-starting bi-chromatic linbo3 soliton microcomb,” *Optica* **6**, 1138 (2019).
- ¹⁸B. Min, T. J. Kippenberg, L. Yang, K. J. Vahala, J. Kalkman, and A. Polman, “Erbium-implanted high-q silica toroidal microcavity laser on a silicon chip,” *Physical Review A* **70**, 033803 (2004).
- ¹⁹L. Agazzi, K. Worhoff, and M. Pollnau, “Energy-transfer-upconversion models, their applicability and breakdown in the presence of spectroscopically distinct ion classes: A case study in amorphous al2o3: Er3+,” *The Journal of Physical Chemistry C* **117**, 6759–6776 (2013).
- ²⁰J. Mu, M. Dijkstra, J. Korterik, H. Offerhaus, and S. M. García-Blanco, “High-gain waveguide amplifiers in si3n4 technology via double-layer monolithic integration,” *Photonics Research* **8**, 1634–1641 (2020).
- ²¹J. Rönn, J. Zhang, W. Zhang, Z. Tu, A. Matikainen, X. Leroux, E. Durán-Valdeiglesias, N. Vulliet, F. Boeuf, C. Alonso-Ramos, *et al.*, “Erbium-doped hybrid waveguide amplifiers with net optical gain on a fully industrial 300 mm silicon nitride photonic platform,” *Optics Express* **28**, 27919–27926 (2020).
- ²²S. A. Vázquez-Córdova, M. Dijkstra, E. H. Bernhardt, F. Ay, K. Wörhoff, J. L. Herek, S. M. García-Blanco, and M. Pollnau, “Erbium-doped spiral amplifiers with 20 db of net gain on silicon,” *Optics Express* **22**, 25993–26004 (2014).
- ²³J. Rönn, W. Zhang, A. Autere, X. Leroux, L. Pakarinen, C. Alonso-Ramos, A. Säynätjoki, H. Lipsanen, L. Vivien, E. Casan, *et al.*, “Ultra-high on-chip optical gain in erbium-based hybrid slot waveguides,” *Nature Communications* **10**, 1–9 (2019).
- ²⁴Y. Liu, X. Yan, J. Wu, B. Zhu, Y. Chen, and X. Chen, “On-chip erbium-doped lithium niobate microcavity laser,” *SCIENCE CHINA Physics, Mechanics & Astronomy* **64**, 1–5 (2021).
- ²⁵Z. Wang, Z. Fang, Z. Liu, W. Chu, Y. Zhou, J. Zhang, R. Wu, M. Wang, T. Lu, and Y. Cheng, “On-chip tunable microdisk laser fabricated on er3+-doped lithium niobate on insulator,” *Optics Letters* **46**, 380–383 (2021).
- ²⁶D. Yin, Y. Zhou, Z. Liu, Z. Wang, H. Zhang, Z. Fang, W. Chu, R. Wu, J. Zhang, W. Chen, *et al.*, “Electro-optically tunable microring laser monolithically integrated on lithium niobate on insulator,” *Optics Letters* **46**, 2127–2130 (2021).
- ²⁷Q. Luo, C. Ya, R. Zhang, Z. Hao, D. Zheng, H. Liu, X. Yu, F. Gao, F. Bo, Y. Kong, *et al.*, “On-chip erbium-doped lithium niobate microring lasers,” *arXiv preprint arXiv:2103.09558* (2021).
- ²⁸Q. Luo, Z. Z. Hao, C. Yang, R. Zhang, and J. J. Xu, “Microdisk lasers on an erbium-doped lithium-niobite chip,” *Science China: Physics, Mechanics and Astronomy* **64** (2021).
- ²⁹Z. Chen, Q. Xu, K. Zhang, W.-H. Wong, D.-L. Zhang, E. Y.-B. Pun, and C. Wang, “Efficient erbium-doped thin-film lithium niobate waveguide amplifiers,” *Optics Letters* **46**, 1161–1164 (2021).
- ³⁰J. Zhou, Y. Liang, Z. Liu, W. Chu, H. Zhang, D. Yin, Z. Fang, R. Wu, J. Zhang, W. Chen, *et al.*, “On-chip integrated waveguide amplifiers on erbium-doped thin film lithium niobate on insulator,” *arXiv preprint arXiv:2101.00783* (2021).
- ³¹Q. Luo, C. Yang, Z. Hao, R. Zhang, D. Zheng, F. Bo, Y. Kong, G. Zhang, and J. Xu, “On-chip erbium-doped lithium niobate waveguide amplifiers,” *arXiv preprint arXiv:2103.15786* (2021).
- ³²D. L. Zhang, F. Han, B. Chen, P. R. Hua, D. Y. Yu, and Y. B. Pun, “Optical-damage-resistant highly er -doped ti:er:linbo strip waveguide,” *Journal of Lightwave Technology* **32**, 135–140 (2013).
- ³³D. Brüske, S. Suntsov, C. Rüter, and D. Kip, “Efficient ridge waveguide amplifiers and lasers in er-doped lithium niobate by optical grade dicing and three-side er and ti in-diffusion,” *Optics Express* **25**, 29374 (2017).